Desalination and Water Treatment
www.deswater.com
doi: 10.5004/dwt.2020.25445

194 (2020) 411–416
August

Thorium adsorption by oxidized biochar pine needles - the effect of particle size

K. Philippou*, A. Konstantinou, I. Pashalidis

Department of Chemistry, University of Cyprus, P.O. Box: 20537, Cy-1678 Nicosia, Cyprus, emails: kphili03@ucy.ac.cy (K. Philippou), konstantinou.athina@ucy.ac.cy (A. Konstantinou), pspasch@ucy.ac.cy (I. Pashalidis)

Received 6 August 2019; Accepted 27 December 2019

ABSTRACT

Removal and recovery of economically important (radio) toxic metals from industrial process and wastewaters is of particular interest in the frame of environmental protection and the need to cover the growing demand for sustainable energy production. Thorium (Th-232) is a potential primary fuel in the nuclear industry, it can be used in different reactor types and has compared to uranium important waste disposal and proliferation advantages. The present study deals with adsorption/removal of Th(IV) from aqueous solutions and particularly the effect of particle size on the metal ion adsorption by oxidized biochar fibers derived from pine needles. The adsorption experiments were performed by batch-type experiments and include the effect of particle size on the adsorption capacity (q_{max}) and adsorption kinetics (k_1), as well as Fourier transform infrared spectroscopy studies and X-ray diffraction measurements for the characterization of adsorbed species and solid phases, respectively. The experimental data indicate that there is an optimum range of particle size in which maximum values for the adsorption capacity (q_{max} = 0.76 mol kg^{-1} or 176 g kg^{-1}) and the kinetic constant (k_1 = 0.3 s^{-1}) are observed. Generally, the experimental adsorption data were found to be well fitted with the Langmuir isotherm and the adsorption kinetics has been evaluated using the Lagergren pseudo-first-order model. Moreover, thermodynamic measurements indicate that the Th(IV) adsorption by oxidized pine needles biochar is an entropy-driven process.

Keywords: Oxidized biochar; Th(IV); Adsorption; Particle size; Aqueous solutions

1. Introduction

Removal and recovery of economically important metals from industrial processes and wastewaters is of particular interest in the frame of environmental protection and the need to cover the growing demand for metals that play a key role in green and sustainable energy production and manufacturing [1,2]. Various techniques have been developed to remove (radio) toxic metals (e.g. Th(IV)) from contaminated waters, including chemical oxidation, electrocoagulation, solvent extraction and adsorption [1,2]. Amongst the various techniques that have been developed for the recovery of metal ions from aqueous systems, adsorption and specifically biosorption are the methods of choice for wastewater remediation and metal-ion recovery due to its simplicity, low cost and efficiency [1–3]. Many types of adsorbents were developed and applied for the recovery of thorium from aqueous media such as algae [4], bacteria [5], plant biomass [6,7], zeolites [8,9], activated carbons [10,11] and graphene oxide [12]. Generally, the experiments were performed at pH values between 3.0 and 6.5 and the adsorption capacity was found to be between 9.4 and 195.7 mg g^{-1}. In addition, the experimental data were better fitted with the Langmuir isotherm and the pseudo-second-order kinetic models. Over the last decade, there is increased interest in the use of biochar fibers, which present remarkable adsorbent properties, such

* Corresponding author.

Presented at the 7th International Conference on Sustainable Solid Waste Management, 26–29 June 2019, Heraklion, Crete Island, Greece

as easy material transport and high external surface available for adsorption. In addition, their affinity can be enhanced towards hard metal ions after oxidation and the formation of surface carboxylic moieties [10–15]. Furthermore, compared to other adsorbent materials, biochars have relatively lower production costs, are environmentally friendly and in line with a circular economy approach.

The present study is focused on thorium (Th) because this actinide is a potential primary fuel in the nuclear industry and can be used as an alternative to uranium (U-235), because of its important waste disposal and proliferation advantages [16]. Hence, anthropogenic activities related to the thorium fuel cycle, which is associated with large volumes of process and wastewaters containing thorium, could result in the environmental pollution in the near field of such activities [17]. The experiments have been carried out with Th(IV) because tetravalent thorium (Th(IV)) is the predominant oxidation state in aqueous systems [10,18]. There are few studies related to Th(IV) adsorption by biochar fibers, which have been focused on the effect of various physicochemical parameters (e.g. pH, metal ion concentration, temperature, contact time, ionic strength) affecting the adsorption efficiency. These studies include Th(IV) adsorption from aqueous solution by oxidized biochar fibers derived from *Luffa cylindrica* [10], olive pulp and olive stone [9,19], cactus fibers [11], as well as graphene oxides [12]. However, to the best of our knowledge, there are no investigations dealing with the effect of biochar particle size on the adsorption efficiency. Hence the present study deals with the adsorption of Th(IV) from aqueous solutions and in particular with the effect of particle size on the adsorption efficiency of thorium by oxidized biochar fibers derived from pine needles (pnco).

2. Experimental

The adsorption experiments and the determination of thorium concentration in the test solutions were carried out as described elsewhere [10,11,20]. The adsorbent used was oxidized biochar prepared from pine needles (oxidized pine needle biochar, pnco). The pine needles were collected from a locally grown pine tree (*Pinus brutia Pegeia*). The washed and air-dried needles were thermally treated under anoxic conditions (N_2) to obtain the carbonized product. The biochar was then oxidized with concentrated nitric acid (8 M HNO_3, 3 h) and prepared for the characterization studies Fourier transform infrared spectroscopy (FTIR), X-ray diffraction (XRD) as described elsewhere [7,12,14]. The different biochar particle fractions were obtained by using sieves of different mesh sizes (>500 μm, 500–200 μm, 200–100 μm, 100–50 μm and <50 μm).

Thorium adsorption on the oxidized biochar was investigated by batch equilibrium experiments as described elsewhere [10,11] at pH 3, total volume of solution (0.03 L), constant mass of the biochar (m = 0.01 g/0.03 L) and variable initial metal ion concentration (5×10^{-6} mol L^{-1} < [Th(IV)] < 5×10^{-3} mol L^{-1}). For the kinetic experiment pH, initial metal ion concentration and mass of the biochar were kept constant and the contact time was between 0 and 1,440 min). The data analysis, as well as the uncertainty evaluation, was carried out as described elsewhere [10,20]. The relative amount of metal ion adsorbed was determined using the following Eq. (1):

$$(\%)\ \text{rel. adsorption} = 100 \times \frac{\left(\left[\text{Th(IV)}\right]_0 - \left[\text{Th(IV)}\right]_{aq}\right)}{\left[\text{Th(IV)}\right]_0} \quad (1)$$

where $[Th(IV)]_o$ = the total metal ion concentration (mol L^{-1}) in the system or in the reference solution, $[Th(IV)]_{aq}$ = metal ion concentration (mol L^{-1}) in the test solution. In addition, at equilibrium conditions [Th(IV)] is similar to C_e (mol L^{-1}) and q corresponds to the amount of Th(IV), adsorbed per unit mass of adsorbent.

The effect of temperature and contact time in order to evaluate the thermodynamic and kinetic parameters $\Delta H°$ and $\Delta S°$, and k_1, respectively, was carried out using 30 mL aqueous solutions containing 0.01 g of the adsorbent and 5×10^{-4} M Th(IV) at pH 3. Evaluation of the thermodynamic parameters was performed using Eqs. (2) and (3):

$$\ln K_d = -\frac{\Delta H°}{RT} + \frac{\Delta S°}{R} \quad (2)$$

and

$$K_d = \frac{\left(\left[\text{Th(IV)}\right]_0 - \left[\text{Th(IV)}\right]_e\right)}{\left[\text{Th(IV)}\right]_e} \times \frac{V}{m} \quad (3)$$

where K_d is the distribution coefficient, $\Delta H°$ and $\Delta S°$ the standard enthalpy and entropy, respectively, T the temperature in K, R is the universal gas constant, V the solution volume and m the mass of the adsorbent.

The adsorption experimental data have been fitted using the Langmuir isotherm. The Langmuir isotherm model is based on the assumption that all surface sites are similar and independent of their neighboring site occupancy. Since Th(IV) adsorption is expected to take place on specific surface-active groups (e.g. carboxylic groups) forming inner-sphere complexes [10,11], the Langmuir isotherm model is expected to fit well the experimental data. Moreover, the maximum adsorption capacity q_{max} is expected to coincide with the maximum number of surface sites available for adsorption. The Langmuir isotherm model can be described by Eq. (4):

$$q = \frac{q_{max} \times K_L \times C_e}{1 + K_L \times C_e} \quad (4)$$

where q_{max} is the maximum monolayer adsorption capacity (mg g^{-1}) and K_L is the Langmuir isotherm constant (L mg^{-1}) related to adsorption energy [21,22].

3. Results and discussion

3.1. Th(IV) adsorption by oxidized pine needle biochar (pnco)

The adsorption of Th(IV) by oxidized biochar fibers have been previously investigated using oxidized biochar fibers obtained from *Opuntia ficus-indica* and *Luffa cylindrica* plant fibers [10,11]. The adsorption experiments have been

performed at pH 3 to avoid hydrolysis reactions resulting in the formation of Th(IV) colloidal species and $Th(OH)_4$ surface precipitation. The experimental data have shown increased adsorption of thorium, which was ascribed to the formation of inner-sphere complexes between Th(IV) and the carboxylic groups present on the biochar surface [10,11]. Similarly, the interaction of Th(IV) with oxidized pine needle biochar (pnco) results in the formation of inner-sphere complexes as indicated by the corresponding IR spectra in Fig. 1. The peaks at 3,443 and 1,705 cm^{-1} are attributed to the stretching vibrations of O–H associated with the carboxylic moieties or adsorbed water and the carboxylic moiety (C=O), respectively. The peak at 1,630 cm^{-1} corresponds to the bending vibrations of adsorbed water molecules, whereas the peak at 1,611 to the stretching vibrations the carboxylic C–O moiety v(C–O). Moreover, the peaks observed at 1,369; 1,241; 1,098; and 614 cm^{-1} are observed due to the bending vibrations of C–O and C–H groups, respectively [10,11].

The significant changes in the peak ratio at 1,705 and 1,611 cm^{-1} with increasing initial metal concentration indicate the formation of inner-sphere surface complexes between Th(IV) and the surface carboxylic moieties as schematically described by a reaction in Fig. 2:

The Th(IV) adsorption is expected to occur via cation exchange reactions, as described by Eq. (1) because at pH 3 the carboxylic moieties are protonated and Th(IV) is expected to be present as cationic di-hydroxy complex [18].

3.2. Effect of particle size on the adsorption capacity

The adsorption capacity of the oxidized biochar regarding Th(IV) adsorption has been investigated as a function of the pnco particle size by batch-type equilibrium experiments. The related experimental data are shown in Fig. 3 and indicate that the pnco fraction with particle size between 100 and 200 μm presents significantly higher adsorption capacity than the other fractions. This could be attributed to the fact at this particle fraction the oxidized biochar offers the highest surface available for adsorption since the particles are small enough but do not stick with one another, resulting in lower specific surface area.

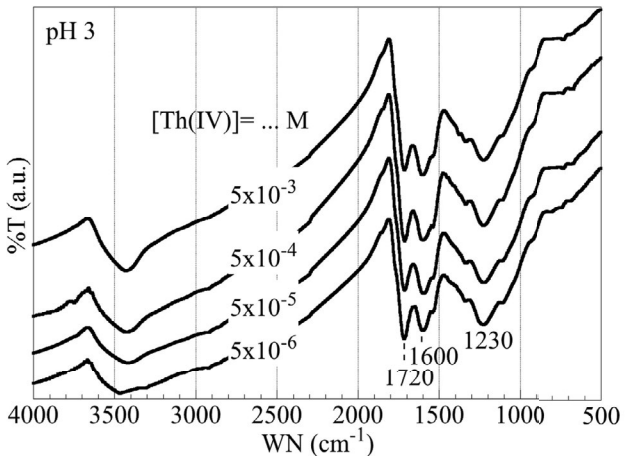

Fig. 1. FTIR spectra of the oxidized biochar after Th(IV) adsorption at pH 3.0 and at different thorium concentrations.

The evaluation of the maximum adsorption capacities (q_{max}) has been carried out by applying the Langmuir adsorption isotherm model to the experimental data and the q_{max} values obtained are summarized in Table 1.

The q_{max} value of the biochar fraction between 100 and 200 μm is generally higher than q_{max} values found in the literature for Th(IV) adsorption by biomasses and carbonaceous materials [4,6,7,10–12,19,23,24], especially under such an acidic environment (Table 2).

In order to prove that no surface precipitation has occurred, XRD measurements have been performed and the corresponding diffractograms are presented in Fig. 4. According to Fig. 4, only the characteristic broad peaks of biochar are observed and there is no indication of Th(IV) solid-phase precipitation up to a thorium concentration of 5×10^{-3} mol L^{-1}, at pH 3.

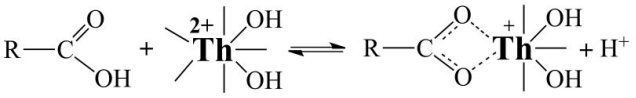

Fig. 2. Structure of inner-sphere surface complexes between Th(IV) and the surface carboxylic moieties.

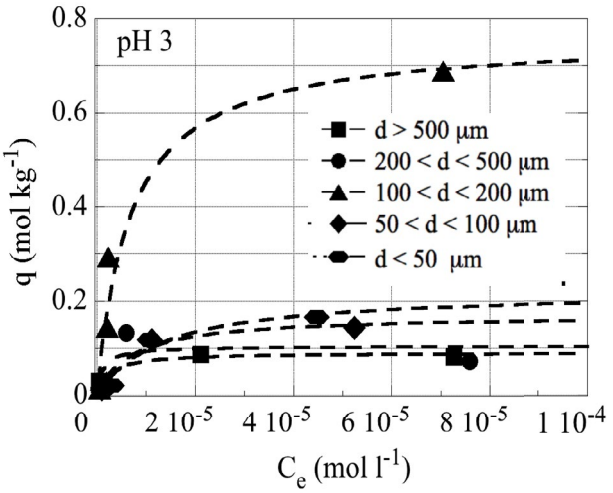

Fig. 3. Adsorption isotherms of Th(IV) adsorption on oxidized pine needle biochar (pnco) as a function of the biochar particle size at pH 3 (0.01 g of biochar, V = 30 mL, $[Th(IV)]_o$ = 5×10^{-6}–5×10^{-3} mol L^{-1}, T = 23°C ± 2°C, 3 d reaction time).

Table 1
Maximum adsorption capacities (q_{max}) for the Th(IV) adsorption by pnco as a function of the particle size fraction

Particle fraction (μm)	q_{max} (moL kg^{-1})	R
>500	0.09	0.94
500–200	0.10	0.79
200–100	0.76	0.97
100–50	0.17	0.98
<50	0.22	0.98

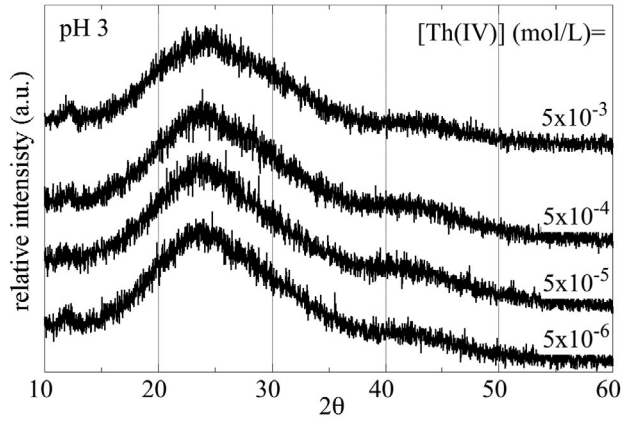

Fig. 4. XRD spectra of the oxidized biochar after Th(IV) adsorption at pH 3 and at different thorium concentrations.

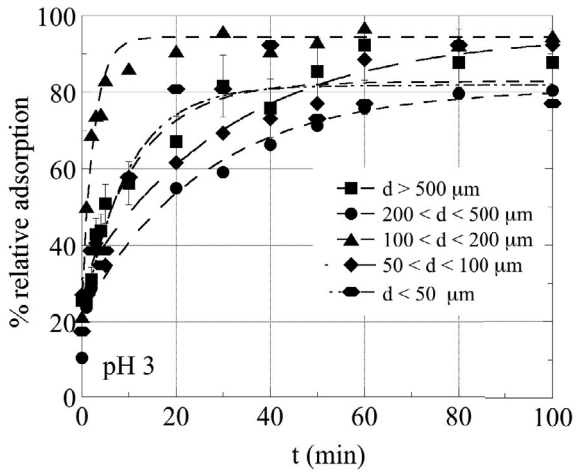

Fig. 5. Relative adsorption of Th(IV) by oxidized pine needle biochar as a function of time and for different biochar fractions at pH 3 (0.03 g of biochar, V = 100 mL, $[Th(IV)]_o$ = 5 × 10^{-4} mol L^{-1}, T = 23°C ± 2°C).

3.3. Effect of pnco particle size on the adsorption kinetics

The adsorption of Th(IV) by oxidized biochar fibers is a relatively fast two-step process (Fig. 5), whereby the first step corresponds to the interaction of the Th(IV) cations with the surface carboxylic moieties and the second step the metal ion diffusion within the biochar channels [10,11].

In order to evaluate the adsorption kinetics of the present system for biochar samples of different particle fractions, the Lagergren pseudo-first-order model has been applied to the experimental data corresponding to the first, fast adsorption step [10,11]. The respective graphs are shown in Fig. 6, and the evaluated data are summarized in Table 3. The kinetic constants (k_1) were calculated using the Lagergren Eq. (5):

$$\ln\left(q_e - q_t\right) = \ln q_e - k_1 t \tag{5}$$

where q_e is the adsorbed amount of the metal ion in equilibrium (mol kg^{-1}), q_t is the adsorbed amount of the metal ion at time t (mol kg^{-1}), k_1 is the kinetic constant of the pseudo-first-order kinetic model (min^{-1}) and t is the time (min).

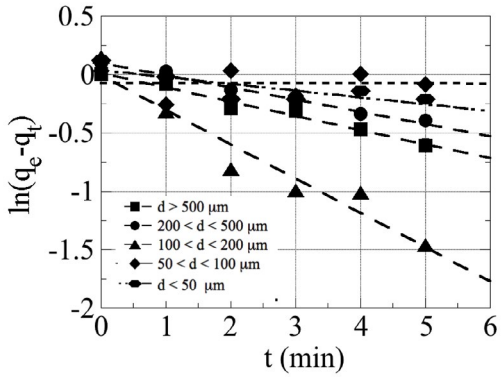

Fig. 6. Lagergren plots corresponding to Th(IV) adsorption on oxidized pine needle biochar (pnco) as a function of the biochar particle size at pH 3 (0.03 g of biochar, V = 100 mL, $[Th(IV)]_o$ = 5 × 10^{-4} mol L^{-1}, T = 23°C ± 2°C).

Table 2
Comparison of adsorption capacities values (q_{max}) of various adsorbent materials for Th(IV)

Adsorbent	pH	q_{max} (mg g^{-1})	R^2	References
Cystoseira indica alga	3.5	195.7	0.99	[4]
Micrococcus luteus Bacteria	6.5	77.0	–	[5]
$CaCl_2$-modified giant kelp biomass	3.5	135.0	0.99	[6]
Nano-iron oxide (Fe_2O_3)-impregnated cellulose acetate composite	6.0	21.3	0.99	[7]
PAN/zeolite composite adsorbent	4.0	9.4	–	[8]
Oxidized biochar fibers derived from *Luffa cylindrica*	3.0	70.0	0.98	[10]
Activated biochar fibers derived from *Opuntia ficus-indica*	3.0	81.0	0.98	[11]
Graphene oxide	2.9	134.6	0.95	[12]
Activated carbon from olive stone	4.0	20.2	0.94	[19]
NaOH-modified biomass derived from duckweed	3.0	96.3	0.99	[23]
Reduced graphene oxide	3.0	48.7	0.99	[24]
Oxidized biochar fibers derived from pine needles	3.0	176	0.98	Present study

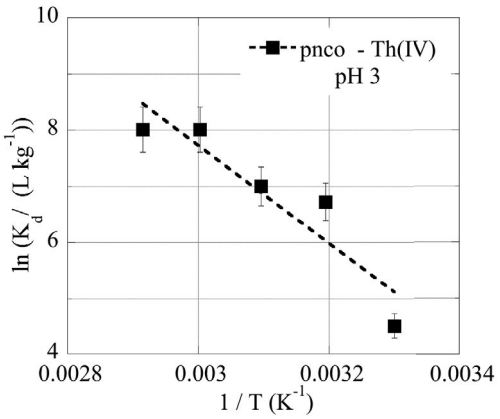

Fig. 7. Effect of temperature, $T(K^{-1})$ on the Th(IV) adsorption by pine needles carbonized-oxidized, pnco at pH 3.

Table 3
Kinetic constants (k_1) for the Th(IV) adsorption by pnco as a function of the particle size fraction

Particle fraction	k_1 (s^{-1})	R
>500	0.1	0.99
500–200	0.1	0.99
200–100	0.3	0.97
100–50	0.01	0.79
<50	0.05	0.80

Based on the experimental results summarized in Table 3, it is obvious that the particle size affects significantly the adsorption rate. Nevertheless, the values of the k_1 are in the range of corresponding values obtained from other thorium adsorption systems found in the literature [11,24].

3.4. Thermodynamic characteristics of the Th(IV) adsorption

The effect of temperature on the Th(IV) adsorption by pnco at the optimum particle size (100–200 μm) was investigated to evaluate the corresponding thermodynamic parameters ($\Delta H°$, $\Delta S°$) using the van't Hoff equation [25]. The experimental data, which are graphically shown in Fig. 7, indicate that with increasing temperature the relative adsorption is increased, assuming that the Th(IV) adsorption is an endothermic ($\Delta H°$ = 73 kJ mol^{-1}) and entropy-driven spontaneous process ($\Delta S°$ = 282 J K^{-1} mol^{-1}).

4. Conclusion

The adsorption capacity of pnco for Th(IV) and the corresponding adsorption rates depend strongly on the biochar particle size. The optimum range of particle size in which the maximum values for the adsorption capacity (q_{max} = 0.76 mol kg^{-1} or 176 g kg^{-1}) and the kinetic constant (k_1 = 0.3 s^{-1}) are observed is between 200–100 μm. According to FTIR studies, the adsorption occurs through the formation of inner-sphere complexes between Th(IV) and the carboxylic groups present on the biochar surface. XRD measurements indicate that there is no surface precipitation of $Th(OH)_4$ and the increased adsorption capacity is attributed to microchannels present in the pine needle biochar, which provide them large external surface available for adsorption. In addition, thermodynamic studies indicate that the Th(IV) adsorption is an endothermic and entropy-driven process ($\Delta S°$ = 282 J K^{-1} mol^{-1}).

References

[1] H.P.S.A. Khalil, A.H. Bhat, A.F.I. Yusra, Green composites from sustainable cellulose nanofibrils: a review, Carbohydr. Polym., 87 (2012) 963–979.
[2] I. Michalak, K. Chojnacka, A. Witek-Krowiak, State of the art for the biosorption process—a review, Appl. Biochem. Biotechnol., 170 (2013) 1389–1416.
[3] C.R.T. Tarley, M.A.Z. Arruda, Natural adsorbents: potential and applications of natural sponge (*Luffa cylindrica*) in lead removal in wastewater laboratory, Rev. Anal., 4 (2003) 26–31.
[4] M. Riazi, A.R. Keshtkar, M.A. Moosavian, Batch and continuous fixed-bed column biosorption of thorium(IV) from aqueous solutions: equilibrium and dynamic modeling, J. Radioanal. Nucl. Chem., 301 (2014) 493–503.
[5] A. Nakajima, T. Tsuruta, Competitive biosorption of thorium and uranium by *Micrococcus luteus*, J. Radioanal. Nucl. Chem., 260 (2004) 13–18.
[6] L. Zhou, Y. Wang, H. Zou, X. Liang, K. Zeng, Z. Liu, A.A. Adesina, Biosorption characteristics of uranium(VI) and thorium(IV) ions from aqueous solution using $CaCl_2$-modified Giant Kelp biomass, J. Radioanal. Nucl. Chem., 307 (2016) 635–644.
[7] P.D. Bhalara, D. Punetha, K. Balasubramanian, Kinetic and isotherm analysis for selective thorium(IV) retrieval from aqueous environment using eco-friendly cellulose composite, Int. J. Environ. Sci. Technol., 12 (2015) 3095–3106.
[8] A. Kilincarslan Kaygun, S. Akyil, Study of the behavior of thorium adsorption on PAN/zeolite composite adsorbent, J. Hazard. Mater., 147 (2007) 357–362
[9] M. Metaxas, V. Kasselouri-Rigopoulou, P. Galiatsatou, C. Konstantopoulou, D. Oikonomou, Thorium removal by different adsorbents, J. Hazard. Mater., 97 (2003) 71–82.
[10] I. Liatsou, E. Christodoulou, I. Pashalidis, Thorium adsorption by oxidized biochar fibers derived from *Luffa cylindrica* sponges, J. Radioanal. Nucl. Chem., 311 (2018) 871–875.
[11] L. Hadjittofi, I. Pashalidis, Thorium removal from acidic aqueous solutions by activated biochar derived from cactus fibers, Desal. Water Treat., 57 (2016) 27864–27868.
[12] Y. Li, C. Wang, Z. Guo, C. Liu, W. Wu, Sorption of thorium(IV) from aqueous solutions by graphene oxide, J. Radioanal. Nucl. Chem., 299 (2014) 1683–1691.
[13] I. Liatsou, P. Constantinou, I. Pashalidis, Copper binding by activated biochar fibers derived from *Luffa cylindrica*, Water Air Soil Pollut., 228 (2017) 255.
[14] I. Liatsou, G. Michail, M. Demetriou, I. Pashalidis, Uranium binding by biochar fibers derived from *Luffa cylindrica* after controlled surface oxidation, J. Radioanal. Nucl. Chem., 311 (2017) 871–875.
[15] L. Hadjittofi, M. Prodromou, I. Pashalidis, Activated biochar derived from cactus fibers – preparation, characterization, and application on Cu(II) removal from aqueous solutions, Bioresour. Technol., 159 (2014) 460–464.
[16] IAEA: Thorium Fuel Utilization: Options and Trends, Proceedings of Three IAEA Meetings held in Vienna in 1997, 1998 and 1999, IAEA-TECDOC-1319, Vienna, 2002.
[17] B.L.K. Somayajulu, E.D. Goldberg, Thorium and uranium isotopes in seawater and sediments, Earth Planet. Sci. Lett., 1 (1966) 102–106.
[18] Th. Fanghänel, V. Neck, Aquatic chemistry and solubility phenomena of actinide oxides/hydroxides, Pure Appl. Chem., 74 (2002) 1895–1907.
[19] C. Kutahyali, M. Eral, Sorption studies of uranium and thorium on activated carbon prepared from olive stones: kinetic and thermodynamic aspects, J. Nucl. Mater., 396 (2010) 251–256.

[20] K. Philippou, I. Savva, I. Pashalidis, Uranium(VI) binding by pine needles prior and after chemical modification, J. Radioanal. Nucl. Chem., 318 (2018) 2205–2211.
[21] D. Hritcu, D. Humelnicu, G. Dodi, M.I. Popa, Magnetic chitosan composite particles: evaluation of thorium and uranyl ion adsorption from aqueous solutions, Carbohydr. Polym., 87 (2012) 1185–1191.
[22] P. Paschalidou, I. Liatsou, I. Pashalidis, C.R. Theocharis, The effect of surface properties on the uranium adsorption by mesoporous ceria, J. Radioanal. Nucl. Chem., 318 (2018) 2193–2197.
[23] T. Chen, N. Zhang, Z. Xu, X. Hu, Z. Ding, Integrated comparisons of thorium(IV) adsorption onto alkali-treated duckweed biomass and duckweed-derived hydrothermal and pyrolytic biochar, Environ. Sci. Pollut. Res., 26 (2019) 2523–2530.
[24] N. Pan, J. Deng, D. Guan, Y. Jin, C. Xia, Adsorption characteristics of Th(IV) ions on reduced graphene oxide from aqueous solutions, Appl. Surf. Sci., 287 (2013) 478–483.
[25] P. Atkins, J. De Paula, Physical Chemistry, Oxford University Press, UK, 2010.